

Structural Insight into BLM Recognition by TopBP1

Luxin Sun¹, Yuhao Huang¹, Ross A. Edwards¹, Sukmin Yang¹, Andrew N. Blackford^{2,3},
Wojciech Niedzwiedz², J.N. Mark Glover^{1,*}

¹Department of Biochemistry, University of Alberta, Edmonton, Alberta, T6G 2H7,
Canada

²Department of Oncology, Weatherall Institute of Molecular Medicine, University of
Oxford, John Radcliffe Hospital, Oxford OX3 9DS, UK

³Cancer Research UK and Medical Research Council Oxford Institute for Radiation
Oncology, University of Oxford, Oxford OX3 7DQ, UK

* Corresponding Author and Lead Contact:

mark.glover@ualberta.ca

telephone: (780) 492-2136

fax: (780) 492-0886

SUMMARY

Topoisomerase II β binding protein 1 (TopBP1) is a critical protein-protein interaction hub in DNA replication checkpoint control. It was proposed that TopBP1 BRCT5 interacts with Bloom syndrome helicase (BLM) to regulate genome stability through either phospho-Ser304 or phospho-Ser338 of BLM. Here we show that TopBP1 BRCT5 specifically interacts with the BLM region surrounding pSer304, not pSer338. Our crystal structure of TopBP1 BRCT4/5 bound to BLM reveals recognition of pSer304 by a conserved pSer-binding pocket, and interactions between a FVPP motif N-terminal to pSer304 and a hydrophobic groove on BRCT5. This interaction utilizes the same surface of BRCT5 that recognizes the DNA damage mediator, MDC1, however the binding orientations of MDC1 and BLM are reversed. While the MDC1 interactions are largely electrostatic, the interaction with BLM has higher affinity and relies on a mix of electrostatics and hydrophobicity. We suggest similar evolutionarily conserved interactions may govern interactions between TopBP1 and 53BP1.

INTRODUCTION

Topoisomerase II β Binding Protein 1 (TopBP1) is a key protein interaction hub that regulates DNA replication, checkpoint activation and damage response ([Garcia et al., 2005](#); [Wardlaw et al., 2014](#)). TopBP1 protein interactions are mediated by its nine BRCA1 associated C-terminus (BRCT) repeats, as well as its ATR activation domain (AAD) that is particularly critical for its role in DNA replication stress signaling which initiates with ATR activation. Although dozens of protein–protein interactions (PPIs) involving the TopBP1 BRCT domains have been reported in the literature, how many of these distinct domains collaborate with different protein partners remains unclear. It has been shown that the N terminal three BRCTs (BRCT0/1/2) of TopBP1 can interact with the phosphorylated Rad9 tail of the Rad9-Hus1-Rad1 (9-1-1) complex to assist ATR-mediated activation of CHK1 in mammalian cells ([Delacroix et al., 2007](#); [Greer et al., 2003](#); [Lee et al., 2007](#)). The C-terminal BRCT7/8 next to the AAD can bind to phosphorylated ATR and has been suggested to help TopBP1 to facilitate ATR kinase activity and substrate binding ([Liu et al., 2011](#)). This BRCT7/8 also interacts with BRCA1 associated C-terminal helicase/Fanconi Anemia J group proteins (BRIP1/FANCD1). This subsequently extends single stranded DNA regions and enhances replication protein A (RPA) loading at stalled replication forks ([Gong et al., 2010](#)).

The internal BRCT5 has been implicated in TopBP1 recruitment to sites of DNA damage under certain circumstances ([Cescutti et al., 2010](#); [Yamane et al., 2002](#)) and several DNA damage-associated proteins have been suggested to interact with this domain in a phosphorylation-dependent manner. The first potential partner identified for BRCT5 was 53BP1, whose interaction was suggested to mediate recruitment of TopBP1 to sites of DNA double strand breaks (DSBs) during G1 ([Cescutti et al., 2010](#); [Yamane et al., 2002](#)). Another DNA double strand break mediator, MDC1, has also been shown to interact with BRCT5, via phosphorylated Ser-Asp-Thr (SDT) repeats in MDC1 ([Leung et al., 2013](#); [Wang et al., 2011](#)). However, more recent studies have suggested that, in cells, TopBP1 instead binds to MDC1 via BRCT1 ([Blackford et al., 2015](#); [Choi and Yoo, 2016](#)).

Recently, two reports have shown that BRCT5 may also interact with Bloom syndrome, RecQ-like helicase (BLM) in a phosphorylation and cell-cycle dependent manner ([Blackford et al., 2015](#); [Wang et al., 2013](#)). In humans, mutations in BLM cause Bloom syndrome, a disease characterized by growth retardation, immunodeficiency,

1
2
3
4 genomic instability, and cancer predisposition ([German, 1993](#)). Disruption of BLM-
5 TopBP1 interaction in cells leads to elevated sister chromatid exchanges (SCEs) and
6 chromosomal aberrations, features that are commonly found in Bloom syndrome
7 patients ([Blackford et al., 2015](#); [Chaganti et al., 1974](#); [German et al., 1965](#); [Wang et al.,](#)
8 [2013](#)). While some evidence suggests that TopBP1 interacts with BLM pSer338 to
9 stabilize BLM during S phase ([Wang et al., 2013](#)), other evidence has suggested that
10 pSer304 of BLM is more crucial for this interaction, and that TopBP1 has no effect on
11 BLM stability ([Bass et al., 2016](#); [Blackford et al., 2015](#)). Here we use fluorescence
12 polarization to demonstrate that TopBP1 BRCT5 specifically binds phosphopeptides
13 corresponding to the pSer304 region of BLM but not the pSer338 region. The X-ray
14 crystal structure of mammalian TopBP1 in complex with a BLM peptide reveals specific
15 recognition of pSer304 by the phosphate binding pocket of BRCT5 and recognition of
16 the residues N-terminal to pSer304 by a hydrophobic groove and positively charged loop
17 in BRCT5. The same surface is used by BRCT5 to bind a phosphorylated SDT repeat in
18 the DNA damage checkpoint mediator, MDC1, however the orientation of BLM binding is
19 reversed compared to MDC1. We suggest that TopBP1 BRCT5 can engage alternative
20 protein partners to regulate DNA replication checkpoints.
21
22
23
24
25
26
27
28
29
30
31
32
33
34

35 RESULTS

36 *TopBP1 BRCT5 interacts with BLM mainly through pSer304 and not pSer338*

37 To assess the likelihood that either Ser304 or Ser338 could serve as targets for
38 TopBP1 BRCT5, we probed the conservation of sequences in this region in a number of
39 vertebrate organisms (Figure 1A). Both Ser304 and Ser338 belong to the BLM N-
40 terminal domain (1-636) that is largely unstructured and poorly conserved. The
41 alignment shows striking conservation of residues N-terminal to the phosphorylation site
42 of Ser304, with acidic residues conserved at the -7 and -5 positions, and a hydrophobic
43 F(V/I)PP motif conserved from -4 to -1 (Figure 1A). In contrast, there is much poorer
44 sequence conservation around Ser338. To directly investigate TopBP1 BRCT5
45 interactions with peptide targets *in vitro*, we synthesized FITC labeled BLM peptides
46 corresponding to both sites (297-DTDFVPPpSPEEII-309, 331-KEDVLSTpSKDL-341)
47 and tested their ability to interact with TopBP1 BRCT5 using fluorescence polarization
48 (FP) spectroscopy. TopBP1 interacts tightly with pSer304 BLM peptide ($K_D = 3.9 \pm 0.3$
49 μM), but weakly with the pSer338 BLM peptide ($K_D \geq 300 \mu\text{M}$) (Figure 1B). To test
50
51
52
53
54
55
56
57
58
59
60
61
62
63
64
65

whether the interaction between TopBP1 BRCT5 and pSer304 BLM peptide is phosphorylation dependent, we dephosphorylated the pSer304 BLM peptide using λ phosphatase (STAR Methods) and examined its interaction with TopBP1 BRCT5 *in vitro* by FP. The λ phosphatase treated peptide binds TopBP1 BRCT5 much more weakly ($K_D \geq 60 \mu\text{M}$) than the phosphorylated peptide (Figure 1C). In addition, control peptides treated under same condition without phosphatase ($K_D = 2.6 \pm 0.4 \mu\text{M}$) or with heat inactivated phosphatase both bind BRCT5 at similar affinity compared to untreated BLM pSer304 peptide ($K_D = 3.7 \pm 0.8 \mu\text{M}$), indicating the treatment itself did not affect peptide affinity to TopBP1 BRCT5. These results show that the phosphorylation of Ser304 is essential for its interaction with TopBP1 BRCT5.

Crystal structure of TopBP1 BRCT4/5 bound to phosphorylated BLM

To gain molecular insight into the interactions involved in pSer304-dependent BLM recognition by TopBP1, we crystallized and determined the structure of TopBP1 BRCT4/5 bound to a pSer304-containing BLM peptide. Crystallization trials using human TopBP1 BRCT4/5 were unsuccessful, however we were able to crystallize and determine the structure of the murine TopBP1 BRCT4/5 – BLM complex at 2.6 Å resolution (STAR Methods). The murine TopBP1 BRCT4/5 and murine BLM Ser304 regions are highly conserved with the human counterparts and interact with similar affinity (Figure 1A; Supplementary Figure 1). The murine complex crystallizes in $P2_1$ space group with 8 copies of TopBP1 BRCT4/5 per asymmetric unit. There exists a translational crystallographic symmetry between protomers ACBE and HDGF, with BLM bound to only half of these protomers (Figure S2). Comparisons of the unbound (EFGH) and bound (ABCD) structures of BRCT4/5 suggest that the TopBP1 structure is largely unchanged upon peptide binding (averaged root-mean-square deviation [rmsd] $C\alpha = 0.147 \text{ Å}^2$ within each set, $C\alpha = 0.469 \text{ Å}^2$ between the peptide-bound and unbound sets). The structural differences are largely limited to the α_1 - β_2 and β_2 '- β_3 ' loops (Supplementary Figure 2B). The β_2 '- β_3 ' loop directly contacts the BLM peptide, which restrains the loop conformation compared to the TopBP1 protomers with no bound peptide. The differences in the BRCT4 α_1 - β_2 loops are likely caused by differences in crystal packing. The overall structure of murine TopBP1 BRCT4/5 adopts a head-to-head packing that is identical to human TopBP1 BRCT4/5, and nearly all residues involved in the BRCT-BRCT interface are conserved (Supplementary Figure 1A). As suggested in

previous BLM-TopBP1 interaction studies ([Blackford et al., 2015](#); [Wang et al., 2013](#)), our structure shows that TopBP1 interacts with BLM exclusively through its BRCT5 domain (Figure 1D, 2, Figure S2C) and indeed FP measurements indicate that BRCT5 and BRCT4/5 bind the BLM peptide with nearly identical affinities (Figure S3A).

Modeling of TopBP1-BLM binding interaction

The electron density enabled us to model the core of the BLM phosphopeptide sequence ³⁰⁰Phe-Val-Pro-Pro-pSer-Pro³⁰⁵ for each of the peptide-bound TopBP1 BRCT4/5 complexes (Table S1, Figure 1D). All peptide protomers adopt similar interactions with the TopBP1 BRCT5 except peptide O that interacts with two protomers (D and E) due to crystal packing (RMSD of C_α = 0.084 Å² between L, M, N, and C_α = 0.201 Å² with O) (Figure S3B). The BLM peptide adopts a typical left-handed type II polyproline (PPII) helical structure. The phosphate group of BLM pSer304 is bound in the phosphate-binding pocket of TopBP1 BRCT5 through a set of hydrogen-bonding interactions with side chains of Lys707, Ser657 and main chain NH of Q658 that are conserved in other BRCT – phosphopeptide structures ([Leung and Glover, 2011](#)) (Figure 2A). The conserved FVPP motif N-terminal to Ser304 contours through a hydrophobic groove on the surface of BRCT5 that leads to the β₂'-β₃' loop. The tandem prolines at positions -1 and -2 pack against Phe681, the valine at -3 is buried within a hydrophobic pocket formed by residues Phe682, Ala710 and Trp714, and the phenylalanine at -4 packs against Met692 at the center of the β₂'-β₃' loop. The -3 valine and phosphoserine are aligned on the same side of the PPII helix for interactions with the BRCT5 binding groove. Although we were unable to model the conserved Asp-Thr-Asp motif N-terminal to the core sequence due lack of electron density, this acidic motif could potentially interact with basic residues including Arg684, Lys685, Lys689 and Lys690 from the β₂'-β₃' loop, which, together with the phosphate binding pocket, render the peptide-binding surface highly electropositive (Figure 1D). C-terminal to pSer304, the peptide tracks away from BRCT5 and in 3 of the 4 complexes, there is no density observable for the semi-conserved Glu-Glu-Ile-Ile motif. In one of the complexes however, this motif is visible and packs against another BRCT5 in the asymmetric unit (Figures S2C, 3B, D). We conclude that the primary TopBP1 binding determinants within the BLM target peptide is the core ³⁰⁰Phe-Val-Pro-Pro-pSer³⁰⁴ region, while the acidic N-terminal motif (²⁹⁷Asp-Thr-Asp²⁹⁹) may play a secondary role to enhance this interaction.

Comparison of BLM and MDC1 recognition by TopBP1

MDC1 has also been identified as a potential binding partner of TopBP1 BRCT4/5 and the structure of a consensus MDC1 SDT repeat region (GFIPSDpTDVEEE) bound to TopBP1 BRCT4/5 was solved by X-ray crystallography ([Leung et al., 2013](#)). MDC1 interacts with TopBP1 in a manner not observed in other BRCT-peptide structures, with one MDC1 peptide sandwiched between two BRCT4/5 domains. There is no direct interface between the two BRCT4/5 protomers, and most of the MDC1 interaction involves just one of the protomers. Evidence that a TopBP1 dimer binds MDC1 more tightly than a monomer in solution comes from FP binding studies that show the untagged monomeric TopBP1 BRCT4/5 binds MDC1 significantly weaker than dimeric GST-BRCT4/5 or GST-BRCT5 ([Leung et al., 2013](#)) (Table 1). In contrast, both the untagged and GST-tagged forms interact with BLM with similar dissociation constants in the 3-6 μ M range that is significantly higher than MDC1 (Figure S3A, Table 1). This suggests that TopBP1 BRCT4/5 interacts with BLM as a monomer and with much higher affinity than MDC1.

In order to understand how TopBP1 BRCT4/5 interacts with two different partners, we first compared these interactions by superimposition of the structures of the TopBP1-BLM and TopBP1-MDC1 complexes (Figure 2A). The TopBP1 BRCT4/5 structures are quite similar between the two complexes (RMSD of C_{α} = 0.497). The same BRCT5 groove is used to engage the two extended phosphopeptide partners, however, the orientation of the two peptides relative to the BRCT5 binding surface is reversed. To further probe the interactions of the two peptides with TopBP1, we compared the impact on peptide binding of a panel of human TopBP1 BRCT5 mutations using the FP assay (Figure 2B). Mutation of either Ser654 or Lys704 in the phosphate binding pocket (equivalent of S657A and K707A in mouse) causes an 8- to 11-fold reduction in BLM binding affinity, consistent with the role of these residues in hydrogen bonding with the pSer304 (Figure 2C). These same mutations only result in a 3.2- to 3.9-fold reduction of affinity in MDC1 for TopBP1. The reduced importance of this pocket for MDC1 binding is consistent with the structure. In the TopBP1 protomer that makes the most extensive contacts with MDC1, the phosphate binding pocket does not bind a phosphate and instead binds the -3 Asp of MDC1. The -3 Asp only partially mimics a pSer, preserving hydrogen bonding interactions with Ser657 and the main chain NH of Gln658. In the other TopBP1 protomer, the MDC1 pThr is partially docked into the phosphate binding

pocket. Two different pairs of charge reversal mutations within the basic β_2' - β_3' loop (R681E/K682E and K686E/K687E, equivalent of R684E/K685E or K689E/K690E in mouse) reduced TopBP1 affinity ~9- to 12-fold suggesting charged interactions involving this loop are important to stabilize either complex. In the MDC1 complex, the acidic residues at +3 and +4 are in proximity to the β_2' - β_3' loop, while in the BLM complex, we propose it is the DTD motif at positions -5 to -7 that contacts this loop. Both MDC1 and BLM present a valine (position -3 in BLM, position +2 in MDC1) that docks into the TopBP1 hydrophobic pocket (Figure 2A). The floor of this pocket is formed by a conserved alanine (Ala707 in human, Ala710 in mouse). Mutation of this alanine shows strikingly different effects on binding of the two peptides. Replacement of the alanine with either a positive (A707K) or negative (A707D) charge dramatically reduces BLM binding, however only the A707D reduces MDC1 peptide binding. This result suggests that the hydrophobic nature of this pocket is critical for the BLM interaction, but is much less important for the MDC1 interaction. Additional hydrophobic contacts are observed in the BLM complex that is not found in the MDC1 complex (Figure 2A). The BLM proline at -2 docks against TopBP1 Phe681 and the BLM phenylalanine at -4 packs into a shallow hydrophobic depression in the surface of the β_2' - β_3' loop formed by Met692, Val683 and Phe681. Mutations of residues that constitute these surfaces in the human protein (M689A or Y678A) have no appreciable impact on MDC1 binding, however these mutations result in significant reductions in BLM binding (Figure 2B,C).

Taken together, this data indicates that BLM binds TopBP1 BRCT5 in a way that utilizes the electrostatic complementarity between the phosphopeptide and BRCT5, as well as hydrophobic contacts from the PPII helix that impart additional specificity and binding affinity. In contrast, the MDC1-TopBP1 complex appears to be largely electrostatically driven and of much lower affinity than the BLM complex.

DISCUSSION

TopBP1 is distinguished by its range of protein partners that interact with the diverse BRCT domains of TopBP1. TopBP1 BRCT5 has been particularly interesting as it has been proposed to bind multiple phosphoprotein targets: BLM, MDC1 and 53BP1 (although the relevant phosphorylated residue in the latter has not yet been identified). Our work shows that the recognition of BLM is highly specific for the region surrounding pSer304 and likely does not involve pSer338, which was also proposed as a possible

1
2
3
4 binding target ([Wang et al., 2013](#)). While MDC1 recognition involves the same surface
5 on BRCT5, the MDC1 peptide binds in an opposite orientation to that observed for BLM,
6 and is of lower affinity and specificity, relying primarily on electrostatic interactions
7 between the highly negatively charged MDC1 phosphopeptide and the positively
8 charged surface of BRCT5. Our results raise further doubts as to whether MDC1 is a
9 physiological binding partner for BRCT5 of TopBP1 ([Blackford et al., 2015](#); [Choi and](#)
10 [Yoo, 2016](#)), although a similar electrostatic interaction may also explain reports of
11 interactions between BRCT5 and single stranded DNA, which have been suggested to
12 play a role in the recognition of stalled DNA replication forks ([Acevedo et al., 2016](#)).
13
14
15
16
17
18
19

20 TopBP1 BRCT4/5 has not only been shown to interact with BLM and MDC1, but
21 has also been implicated in binding the key DNA damage signaling factor, 53BP1, in a
22 phosphorylation-dependent interaction ([Cescutti et al., 2010](#); [Yamane et al., 2002](#)).
23 Insight into this interaction has been provided by structural studies of the *S. pombe*
24 orthologs of these proteins, Rad4^{TopBP1} and Crb2^{53BP1} ([Qu et al., 2013](#)). Rad4^{TopBP1}
25 contains a pair of BRCTs (BRCT1 and BRCT2) which can both bind either of two
26 Crb2^{53BP1} phosphopeptides containing a VxxpT motif in a manner that is similar to the
27 binding of BLM by TopBP1 BRCT5, both in terms of the left-handed helical tracking of
28 the peptide across the BRCT surface and docking of the -3 Val into the BRCT
29 hydrophobic pocket (Figure 3A). The major difference between TopBP1 BRCT5 and
30 either BRCT1 or BRCT2 of Rad4^{TopBP1} is the lack of the positively charged β_2 '- β_3 ' loop in
31 the Rad4^{TopBP1} BRCTs (Figure 3A,B) and the Crb2 phosphopeptide binding partner does
32 not contain the conserved negatively charged residues at positions -4 to -7 observed in
33 BLM (Figure 3C).
34
35
36
37
38
39
40
41
42
43

44 To probe the possibility that similar interactions might be responsible for TopBP1-
45 53BP1 interactions in the mammalian homologs, we scanned the known 53BP1
46 phosphorylation sites for potential TopBP1 binding sites that contain VxxpS/T motifs.
47 Several sites match this motif with the best matches centering on pSer366 and
48 pSer379/pSer380 (Figure 3C,D). While other 53BP1 phosphosites conform to the
49 VxxpS/T motif, the pSer366 and pSer379/pSer380 sites are flanked by a conserved
50 proline-containing hydrophobic region from -1 to -4 and additional acidic or potentially
51 phosphorylated residues that could provide electrostatic interactions with the β_2 '- β_3 ' loop
52 (Figure 3D).
53
54
55
56
57
58
59
60
61
62
63
64
65

1
2
3
4 Agents that increase the replication stress load in cancer cells are particularly
5 effective chemotherapeutics. Cells in which the BLM-TopBP1 interaction is disrupted
6 show increased replication stress, as evidenced by the increased DNA replication origin
7 firing, chromosomal aberrations and SCEs ([Blackford et al., 2015](#)). Therefore, the
8 structure of the BRCT domains of TopBP1 in complex with a BLM peptide lays the
9 foundation for targeting of the BLM-TopBP1 interaction with small molecules as potential
10 chemotherapeutic agents.
11
12
13
14
15
16
17
18
19

20 **AUTHOR CONTRIBUTIONS**

21
22 L.S. and Y.H. produced all proteins, performed crystallographic analysis, and performed
23 all fluorescence polarization measurements. R.A.E. assisted with crystallographic
24 structure determination and refinement and S.Y. assisted with λ phosphatase
25 experiments. L.S., A.N.B., W.N., and J.N.M.G. conceived the experiments and prepared
26 the manuscript.
27
28
29
30
31
32
33
34

35 **ACKNOWLEDGEMENTS**

36
37
38 We thank Dr. Pawel Grochulski and the staff at the Canadian Light Source CMCF
39 beamline 08ID-1 for assistance with synchrotron data collection. This work was funded
40 by NCI program project grant PO1CA092584 to J.N.M.G, CIHR grant 114975 to J.N.M.G
41 and NSERC Discovery grant 2016-05163 to J.N.M.G. A.N.B. is supported by a Cancer
42 Research UK Career Development Fellowship (C29215/A20772).
43
44
45
46
47
48
49
50
51
52
53
54
55
56
57
58
59
60
61
62
63
64
65

REFERENCES

Acevedo, J., Yan, S., and Michael, W.M. (2016). Direct Binding to Replication Protein A (RPA)-coated Single-stranded DNA Allows Recruitment of the ATR Activator TopBP1 to Sites of DNA Damage. *J Biol Chem* 291, 13124-13131.

Adams, P.D., Afonine, P.V., Bunkoczi, G., Chen, V.B., Davis, I.W., Echols, N., Headd, J.J., Hung, L.W., Kapral, G.J., Grosse-Kunstleve, R.W., *et al.* (2010). PHENIX: a comprehensive Python-based system for macromolecular structure solution. *Acta Crystallogr D Biol Crystallogr* 66, 213-221.

Bass, T.E., Luzwick, J.W., Kavanaugh, G., Carroll, C., Dungrawala, H., Glick, G.G., Feldkamp, M.D., Putney, R., Chazin, W.J., and Cortez, D. (2016). ETAA1 acts at stalled replication forks to maintain genome integrity. *Nat Cell Biol* 18, 1185-1195.

Blackford, A.N., Nieminuszczy, J., Schwab, R.A., Galanty, Y., Jackson, S.P., and Niedzwiedz, W. (2015). TopBP1 interacts with BLM to maintain genome stability but is dispensable for preventing BLM degradation. *Mol Cell* 57, 1133-1141.

Braman, J., Papworth, C., and Greener, A. (1996). Site-directed mutagenesis using double-stranded plasmid DNA templates. *Methods Mol Biol* 57, 31-44.

Cescutti, R., Negrini, S., Kohzaki, M., and Halazonetis, T.D. (2010). TopBP1 functions with 53BP1 in the G1 DNA damage checkpoint. *EMBO J* 29, 3723-3732.

Chaganti, R.S., Schonberg, S., and German, J. (1974). A manyfold increase in sister chromatid exchanges in Bloom's syndrome lymphocytes. *Proc Natl Acad Sci U S A* 71, 4508-4512.

Chen, V.B., Arendall, W.B., 3rd, Headd, J.J., Keedy, D.A., Immormino, R.M., Kapral, G.J., Murray, L.W., Richardson, J.S., and Richardson, D.C. (2010). MolProbity: all-atom structure validation for macromolecular crystallography. *Acta Crystallogr D Biol Crystallogr* 66, 12-21.

Choi, S.H., and Yoo, H.Y. (2016). Mdc1 modulates the interaction between TopBP1 and the MRN complex during DNA damage checkpoint responses. *Biochem Biophys Res Commun* 479, 5-11.

Delacroix, S., Wagner, J.M., Kobayashi, M., Yamamoto, K., and Karnitz, L.M. (2007). The Rad9-Hus1-Rad1 (9-1-1) clamp activates checkpoint signaling via TopBP1. *Genes Dev* 21, 1472-1477.

Emsley, P., and Cowtan, K. (2004). Coot: model-building tools for molecular graphics. *Acta Crystallogr D Biol Crystallogr* 60, 2126-2132.

Garcia, V., Furuya, K., and Carr, A.M. (2005). Identification and functional analysis of TopBP1 and its homologs. *DNA Repair* 4, 1227-1239.

German, J. (1993). Bloom-Syndrome - a Mendelian Prototype of Somatic Mutational Disease. *Medicine* 72, 393-406.

German, J., Archibald, R., and Bloom, D. (1965). Chromosomal Breakage in a Rare and Probably Genetically Determined Syndrome of Man. *Science* 148, 506-507.

Gong, Z., Kim, J.E., Leung, C.C., Glover, J.N., and Chen, J. (2010). BACH1/FANCI acts with TopBP1 and participates early in DNA replication checkpoint control. *Mol Cell* 37, 438-446.

Greer, D.A., Besley, B.D., Kennedy, K.B., and Davey, S. (2003). hRad9 rapidly binds DNA containing double-strand breaks and is required for damage-dependent topoisomerase II beta binding protein 1 focus formation. *Cancer Res* 63, 4829-4835.

Koska, J., Spassov, V.Z., Maynard, A.J., Yan, L., Austin, N., Flook, P.K., and Venkatachalam, C.M. (2008). Fully automated molecular mechanics based induced fit protein-ligand docking method. *J Chem Inf Model* 48, 1965-1973.

Kunkel, T.A. (1985). Rapid and efficient site-specific mutagenesis without phenotypic selection. *Proc Natl Acad Sci U S A* 82, 488-492.

1
2
3
4 Lee, J., Kumagai, A., and Dunphy, W.G. (2007). The Rad9-Hus1-Rad1 checkpoint clamp
5 regulates interaction of TopBP1 with ATR. *J Biol Chem* 282, 28036-28044.
6
7

8
9 Leung, C.C., and Glover, J.N. (2011). BRCT domains: easy as one, two, three. *Cell*
10 *Cycle* 10, 2461-2470.
11
12

13
14 Leung, C.C., Sun, L., Gong, Z., Burkat, M., Edwards, R., Assmus, M., Chen, J., and
15 Glover, J.N. (2013). Structural insights into recognition of MDC1 by TopBP1 in DNA
16 replication checkpoint control. *Structure* 21, 1450-1459.
17
18
19

20
21 Liu, S., Shiotani, B., Lahiri, M., Marechal, A., Tse, A., Leung, C.C., Glover, J.N., Yang,
22 X.H., and Zou, L. (2011). ATR autophosphorylation as a molecular switch for checkpoint
23 activation. *Mol Cell* 43, 192-202.
24
25
26

27 McCoy, A.J., Grosse-Kunstleve, R.W., Adams, P.D., Winn, M.D., Storoni, L.C., and Read,
28 R.J. (2007). Phaser crystallographic software. *J Appl Crystallogr* 40, 658-674.
29
30
31

32 Nelson, M., and McClelland, M. (1992). *Methods Enzymol* 216, 24.
33
34
35

36 Qu, M., Rappas, M., Wardlaw, C.P., Garcia, V., Ren, J.Y., Day, M., Carr, A.M., Oliver,
37 A.W., Du, L.L., and Pearl, L.H. (2013). Phosphorylation-dependent assembly and
38 coordination of the DNA damage checkpoint apparatus by Rad4(TopBP1). *Mol Cell* 51,
39 723-736.
40
41
42

43
44 Sugimoto, M., Esaki, N., Tanaka, H., and Soda, K. (1989). A simple and efficient method
45 for the oligonucleotide-directed mutagenesis using plasmid DNA template and
46 phosphorothioate-modified nucleotide. *Anal Biochem* 179, 309-311.
47
48
49

50
51 Taylor, J.W., Ott, J., and Eckstein, F. (1985). The rapid generation of oligonucleotide-
52 directed mutations at high frequency using phosphorothioate-modified DNA. *Nucleic*
53 *Acids Res* 13, 8765-8785.
54
55
56

57 Terwilliger, T.C., Grosse-Kunstleve, R.W., Afonine, P.V., Moriarty, N.W., Adams, P.D.,
58 Read, R.J., Zwart, P.H., and Hung, L.W. (2008). Iterative-build OMIT maps: map
59
60
61

1
2
3
4 improvement by iterative model building and refinement without model bias. *Acta*
5
6 *Crystallogr D Biol Crystallogr* 64, 515-524.
7
8

9 Vandeyar, M.A., Weiner, M.P., Hutton, C.J., and Batt, C.A. (1988). A simple and rapid
10 method for the selection of oligodeoxynucleotide-directed mutants. *Gene* 65, 129-133.
11
12
13

14 Wang, J., Chen, J., and Gong, Z. (2013). TopBP1 controls BLM protein level to maintain
15 genome stability. *Mol Cell* 52, 667-678.
16
17
18

19 Wang, J., Gong, Z., and Chen, J. (2011). MDC1 collaborates with TopBP1 in DNA
20 replication checkpoint control. *J Cell Biol* 193, 267-273.
21
22
23

24 Wardlaw, C.P., Carr, A.M., and Oliver, A.W. (2014). TopBP1: A BRCT-scaffold protein
25 functioning in multiple cellular pathways. *DNA Repair* 22, 165-174.
26
27
28
29
30

31 Yamane, K., Wu, X., and Chen, J. (2002). A DNA damage-regulated BRCT-containing
32 protein, TopBP1, is required for cell survival. *Mol. Cell. Biol.* 22, 555-566.
33
34
35
36
37
38
39
40
41
42
43
44
45
46
47
48
49
50
51
52
53
54
55
56
57
58
59
60
61
62
63
64
65

FIGURE LEGENDS

Figure 1. BLM interacts with TopBP1 via pSer304, not pSer338.

A. Sequence alignment of BLM orthologs around pSer304 and pSer338. Phosphoserine residues are colored in purple, hydrophobic residues are colored in green, and negatively charged residues are colored in red.

B. TopBP1 BRCT4/5 binds more tightly to BLM pSer304 than BLM pSer338. GST-hTopBP1 BRCT5 protein was titrated against BLM phosphopeptides corresponding to either the pSer304 or pSer338 regions and binding was monitored by fluorescence polarization (FP) spectroscopy.

C. TopBP1 BRCT4/5 binds BLM pSer304 in a phosphorylation dependent manner. BLM pSer304 peptide was dephosphorylated by treatment with λ phosphatase (+) and its interaction with GST-hTopBP1 BRCT5 protein was measure by FP. BLM pSer304 peptide mock-treated without λ phosphatase (-) or with heat inactivated phosphatase (HI) were also included as controls.

D. Structural overview of TopBP1 BRCT4/5 in complex with pSer304 BLM peptide. An electrostatic charge surface is displayed for TopBP1 BRCT4/5 while the modeled BLM phosphopeptide is shown in pink sticks. See also Figure S1-3 and Table S1.

Figure 2. Comparison of TopBP1 recognition of BLM and MDC1.

A. Structural comparison of TopBP1-BLM and TopBP1-MDC1 complexes. Mouse TopBP1-BLM complex (left) and human TopBP1-MDC1 (right) are aligned by their BRCT5 main-chain C α positions. Both TopBP1 BRCT structures are displayed with semi-transparent surface over a grey cartoon, while the BLM peptide is displayed as a pink cartoon and the MDC1 peptide is displayed as a blue cartoon. Key interacting residues are displayed as sticks and hydrogen bonds are indicated by yellow dash-lines. Note that the region in mouse TopBP1 N-terminal to BRCT4/5 is three residues larger than the human protein. As a result, the numbers for homologous residues are three larger for mouse compared to human.

1
2
3
4 B. Comparison of the binding affinities of BLM and MDC1 phosphopeptides for a panel
5 of human TopBP1 BRCT5 variants using FP. WT TopBP1 BRCT5 as well as a panel of
6 eight missense variants were titrated against either BLM phosphopeptide (left) or the
7 MDC1 phosphopeptide (right) and their binding affinities were assessed by FP.
8
9

10
11 C. Effects of human TopBP1 BRCT5 missense mutations on the binding of either MDC1
12 or BLM. The fold increase in K_D is plotted for each BRCT5 variant normalized against the
13 binding affinity for the WT. Results for BRCT5-MDC1 interactions are shown in blue,
14 while the results for BRCT5-BLM interactions are shown in pink. The inset shows the
15 relative difference in K_D between WT BRCT5-MDC1 and WT BRCT5-BLM.
16
17
18
19
20
21
22

23 **Figure 3.** TopBP1 BRCT5 may bind BLM and 53BP1 through similar mechanisms.
24
25

26 A. Structures of Rad4^{TopBP1} BRCT repeats bound to Crb2^{53BP1}. Rad4 BRCT1/Crb2 (left)
27 and Rad4 BRCT2/Crb2 (right) structures (PDB code: 4BU0) are aligned with the
28 TopBP1/BLM complex as in Figure 2A. Both structures have surface and cartoon
29 displayed for Rad4^{TopBP1} (BRCT1 in orange, BRCT2 in green) and only cartoon displayed
30 for Crb2^{53BP1} (blue). Interacting residues are displayed as sticks. Hydrogen bonds are
31 indicated by yellow dash-lines.
32
33
34
35
36

37 B. Sequence alignment of the peptide binding region TopBP1 BRCT5 homologues.
38 Residues from the positively charged β_2' - β_3' loop are colored blue, residues from
39 phosphate binding pocket are colored purple, and residues lining hydrophobic groove
40 are colored green.
41
42
43

44 C. Sequence alignment of BLM, Crb2 and 53BP1 phosphopeptide partners for TopBP1
45 BRCT5. Phosphorylated residues are colored purple, negatively charged residues are
46 colored red and hydrophobic residues are colored green.
47
48
49

50 D. Sequence alignment of potential TopBP1 BRCT5 binding regions in 53BP1
51 homologues. Coloring is as in Figure 3C.
52
53
54
55
56
57
58
59
60
61
62
63
64
65

TABLES

Table 1: Summary of Fluorescence Polarization Results

Protein		TopBP1-peptide K _D (μM)		
TopBP1		MDC1	BLM	
GST-hBRCT5	WT	15 ± 1	285 ± 10	pSer338
			60 ± 10	Ser304
			3.9 ± 0.3	pSer304
	S654A	48 ± 6	33 ± 3	
	K704A	59 ± 6	42 ± 3	
	R681E/K682E	170 ± 10	45 ± 2	
	K686E/K687E	130 ± 20	36 ± 3	
	A707K	12 ± 0.9	70 ± 20	
	A707D	120 ± 10	320 ± 40	
	M689A	15 ± 1	53 ± 4	
	Y678A	21 ± 2	18 ± 2	
hBRCT4/5		100 ± 10	3.2 ± 0.8	pSer304
GST-hBRCT4/5		30 ± 4	6 ± 1	
mBRCT4/5		170 ± 20	6 ± 2	

STAR METHODS

Contact for reagent and resource sharing

Further information and requests for resources and reagents should be directed to and will be fulfilled by the Lead Contact: Mark Glover (mark.glover@ualberta.ca)

Cloning, expression and purification

Human TopBP1 BRCT5 (641-746) and BRCT4/5 (549-746), and mouse TopBP1 BRCT4/5 (553-749) were cloned into pGEX-6P-1 (GE Healthcare). Mutants (Y678A, A707D, A707K, M689A) of human TopBP1 BRCT5 were created from the WT template using QuickChange Lightning site-directed mutagenesis kit (Stratagene) ([Braman et al., 1996](#); [Kunkel, 1985](#); [Nelson and McClelland, 1992](#); [Sugimoto et al., 1989](#); [Taylor et al., 1985](#); [Vandeyar et al., 1988](#)). All the GST fusion proteins were expressed in *Escherichia coli* BL21-Gold cells and purified using glutathione affinity chromatography with glutathione sepharose 4B beads (GE Healthcare) and eluted in elution buffer (20 mM Tris-HCl pH 7.5, 150 mM NaCl, 20 mM reduced glutathione and 0.1% β ME). GST-fusion protein of BRCT5 was purified by Superdex 200 16/60 column in storage buffer (10 mM Tris-HCl pH 8.0, 150 mM NaCl, 1 mM DTT). GST-fusion protein of TopBP1 BRCT4/5 was cleaved with PreScission protease overnight at 4 °C. BRCT4/5 was purified by anion exchange chromatography (buffer A: 50 mM HEPES pH 7.0, 0.1% β ME; buffer B: 50 mM HEPES pH 7.0, 1M NaCl, 0.1% β ME). Residual GST was removed by incubation with glutathione sepharose 4B beads (GE Healthcare) prior to a final purification step on a Superdex 75 26/60 column in storage buffer (10 mM Tris-HCl pH 7.5, 150 mM NaCl, 1 mM DTT).

Crystallization

Mouse TopBP1 BRCT4/5 concentrated to 10 mg/mL was incubated with 3-fold molar excess of BLM peptide (Ac-DTDFVPPpSPEEI-NH₂, Genosphere Biotechnologies) for 2 hours on ice. Crystals of the complex were grown at room temperature using hanging drop vapor diffusion by mixing 1 μ L of protein:peptide complex with 1 μ L of reservoir solution (0.1 M sodium citrate pH 5.4 and 24% PEG 8000). Co-crystals were flash-cooled in reservoir solution supplemented with 20% glycerol.

Data collection and structure determination

1
2
3
4 Data for crystals of the BRCT4/5-pSer304 BLM peptide complex were collected at
5 the CMCF 08ID-1 beamline (Canadian Light Source, Saskatoon). Intensity data were
6 processed by DENZO, scaled and reduced using SCALEPACK ([Adams et al., 2010](#)) to
7 the space group *P21* with unit cell dimensions: $a = 98.62\text{\AA}$, $b = 97.0\text{\AA}$, $c = 127.3\text{\AA}$, $\alpha =$
8 90.0° , $\beta = 94.3^\circ$, $\gamma = 90.0^\circ$ ([Otwinowski and Minor, 1997](#)). The human TopBP1 BRCT4/5
9 structure (PDB ID: 3UEN) was used in PHASER 25.6 to successfully find 8 copies in the
10 asymmetric unit ([McCoy et al., 2007](#)). Model building was carried out in COOT and
11 refined using TLS refinement (peptide bound molecule ABCD and unbound molecule
12 EFGH are grouped separately) in PHENIX ([Adams et al., 2010](#); [Emsley and Cowtan,](#)
13 [2004](#)). The BRCT4/5 molecules are related by translational symmetry (Supplementary
14 Figure 2A). BRCT4/5 molecules A and C lack the N-terminal 549–550 residues, C-
15 terminal 742–746 residues, and α_1 - β_2 loop residues 584–588. Molecules B and D lack
16 the N-terminal 549–550 residues, C-terminal 743–746 residues, and α_1 - β_2 loop residues
17 584–589. The BRCT4/5 molecules were fully refined before building of the four peptides.
18 Peptides were positioned by first docking in the key pSer304 residues using Ligandfit in
19 Phenix, and the rest of peptide chain subsequently built manually in COOT ([Koska et al.,](#)
20 [2008](#)). Peptide chains L and M lack the N-terminal 7 to 5 residues and C-terminal +1 to
21 +5 residues, peptide N lacks the N-terminal 7 to 5 residues and C-terminal +1 to +5
22 residue, and peptide O only lacks the N-terminal 7 to 5 residues. The final model was
23 refined in Phenix at 2.6 Å resolution to R_{work} and R_{free} of 0.219 and 0.256, respectively.
24 The Ramachandran plot contained 96.7% of all residues in the favored region. All the 7
25 Ramachandran outliers come from the two flexible loop regions (β_2' - β_3' loop and α_1 - β_2
26 loop) of TopBP1 BRCT4/5. Data collection and refinement statistics for the structures are
27 listed in Table 1. Models were validated with MolProbity ([Chen et al., 2010](#)). Alignments
28 with structure information were done by PROMAL3D. Bias reduced omit maps were
29 generated by Phenix ([Terwilliger et al., 2008](#)). All structure figures were prepared with
30 PyMOL (Version 1.8, www.pymol.org). Please see supplemental materials for PDB
31 Validation Report.
32
33
34
35
36
37
38
39
40
41
42
43
44
45
46
47
48
49
50
51
52

53 Fluorescence polarization assay

54 FP measurements were carried out using an Envision multi-label plate reader
55 (Perkin Elmer) using 384-well OptiPlates (Perkin Elmer). All pSer304 related BLM
56 peptides (FITC-DTDFVPPpSPEEII-NH₂, Ac-DTDFVPPpSPEEII-NH₂, Ac-
57 DTDFVPPpSPEEIIKK-NH₂, Ac-DFVPPpSPEEII-NH₂) were synthesized and purified by
58
59
60
61
62
63
64
65

Genosphere Biotechnologies. The rest of peptides (FITC-KEDVLSTpSKDL-NH₂, FITC-GFIDpSDpTDVEEEE-NH₂) were synthesized and purified by Biomatik. FP assays were performed by mixing 10 nM FITC-labelled phospho-peptide with freshly concentrated TopBP1 in FP assay buffer (10 mM Tris-HCl pH 7.5, 150 mM NaCl, 1 mM DTT, 0.05 % Tween-20) and incubated for 15 minutes at room temperature. FP measurements were carried out at an excitation wavelength of 485 nm and emission wavelength of 538 nm. Curve fitting and K_D calculations were obtained using PRISM software (GraphPad Prism). K_D values summarized in Table 1 are the average of at least three individual measurements.

Lambda (λ) protein phosphatase treatment

Unphosphorylated Ser304 BLM peptide (FITC-DTDFVPPSPEEII-NH₂) was made by treating pSer304 BLM peptide (FITC-DTDFVPPpSPEEII-NH₂) with λ protein phosphatase (New England Biolabs) for 1 hour at 30 °C in reaction buffer (50 mM Tris-HCl, pH 7.5, 0.1 mM Na₂EDTA, 5 mM DTT, and 0.01% Brij 35, 2 mM MnCl₂). Mock-treated control reaction was carried out in the same reaction buffer lacking λ phosphatase. As an additional control, λ phosphatase was inactivated by heating 1 hour at 65 °C in the presence of 50 mM EDTA. The binding affinities of the peptides for GST-TopBP1 BRCT5 were determined by FP.

Data and software availability

Coordinates and scattering data for the BLM-TopBP1 BRCT4/5 complex have been deposited in the Protein Data Bank (RCSB accession: 5U6K). Intensity data were processed by DENZO, scaled and reduced using SCALEPACK. Initial molecular replacement of our data was done using TopBP1 BRCT4/5 structure (PDB ID: 3UEN) in PHASER 25.6. Model building was carried out in COOT and PHENIX. All structure figures were prepared with PyMOL. FP data were analyzed using GraphPad PRISM. All software resources are listed in the Key Resource Table, and the use of each package in the data analysis is described in the sub-headings of the STAR Methods Table.

SUPPLEMENTAL INFORMATION

Figure S1-3 and Table S1 can be found with this article online.

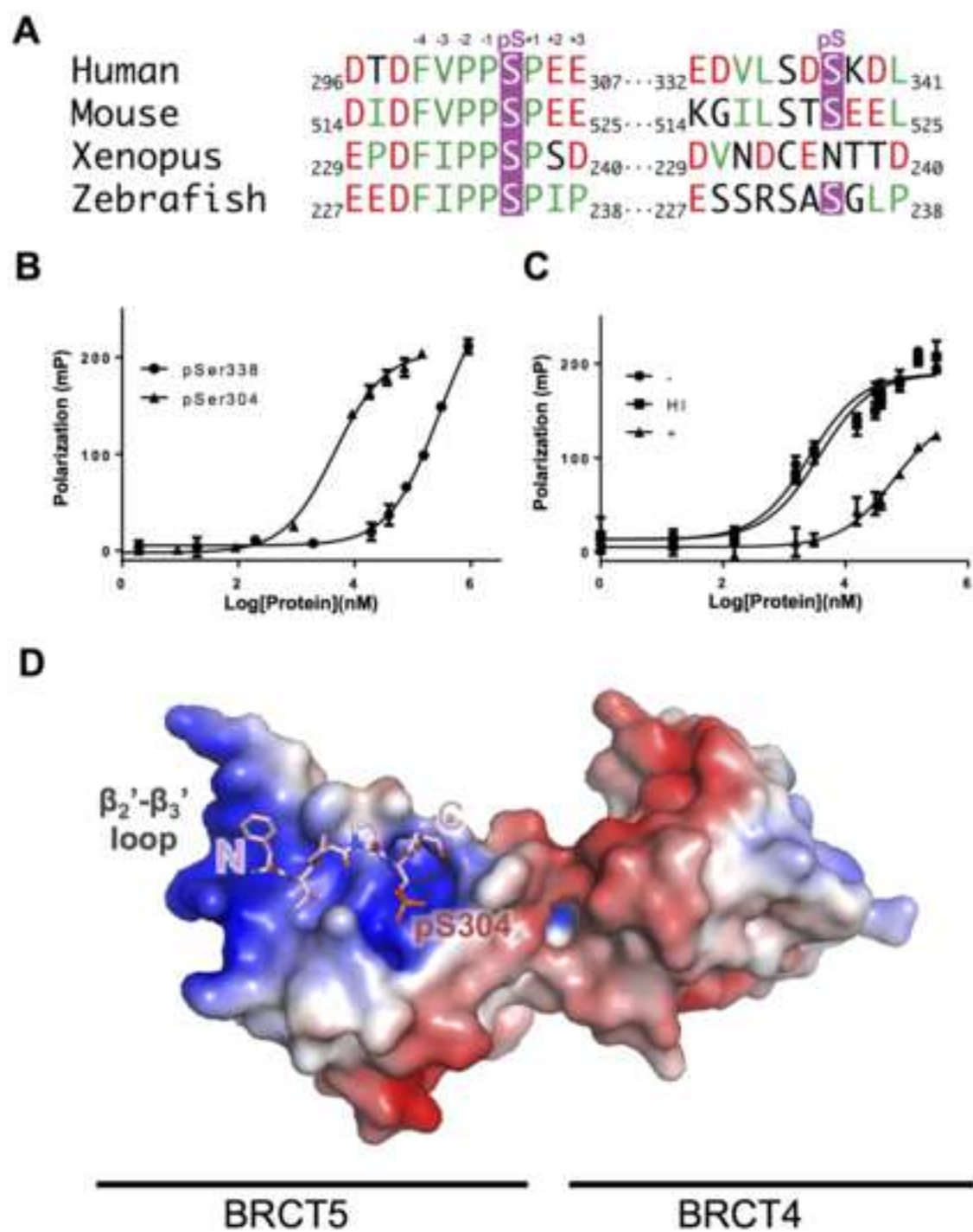
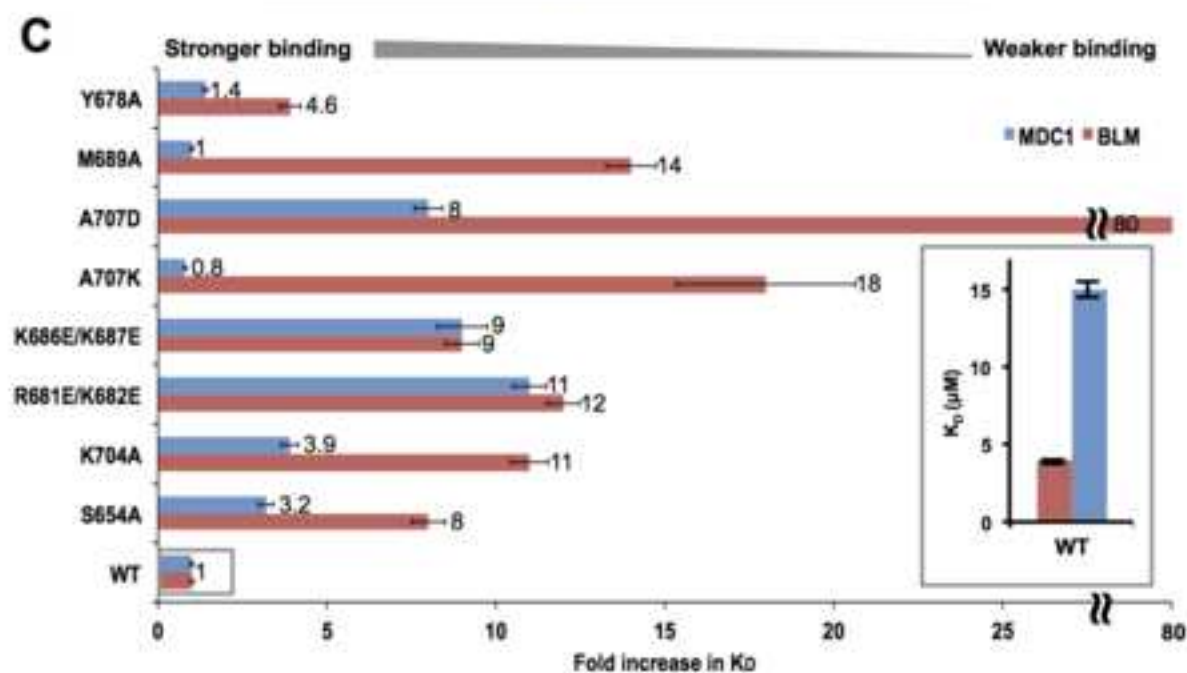
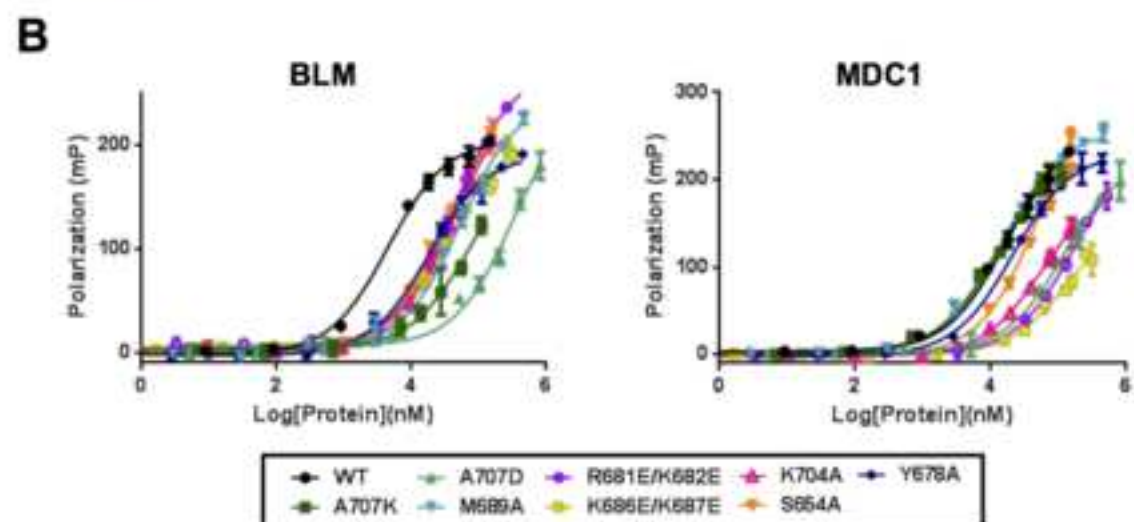
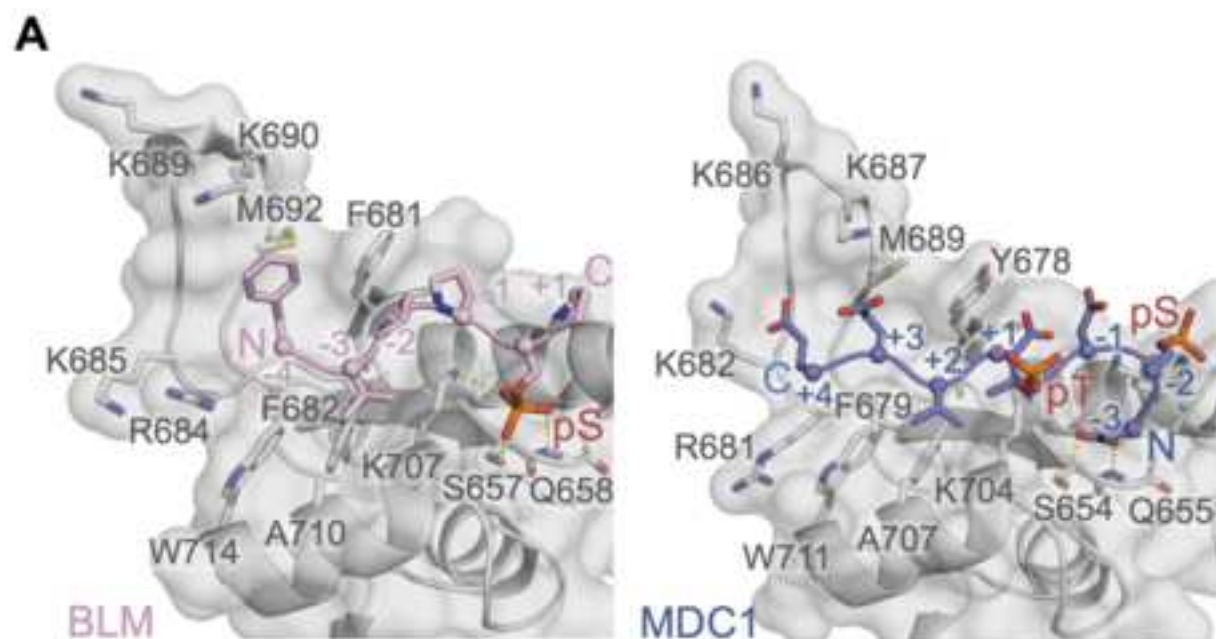
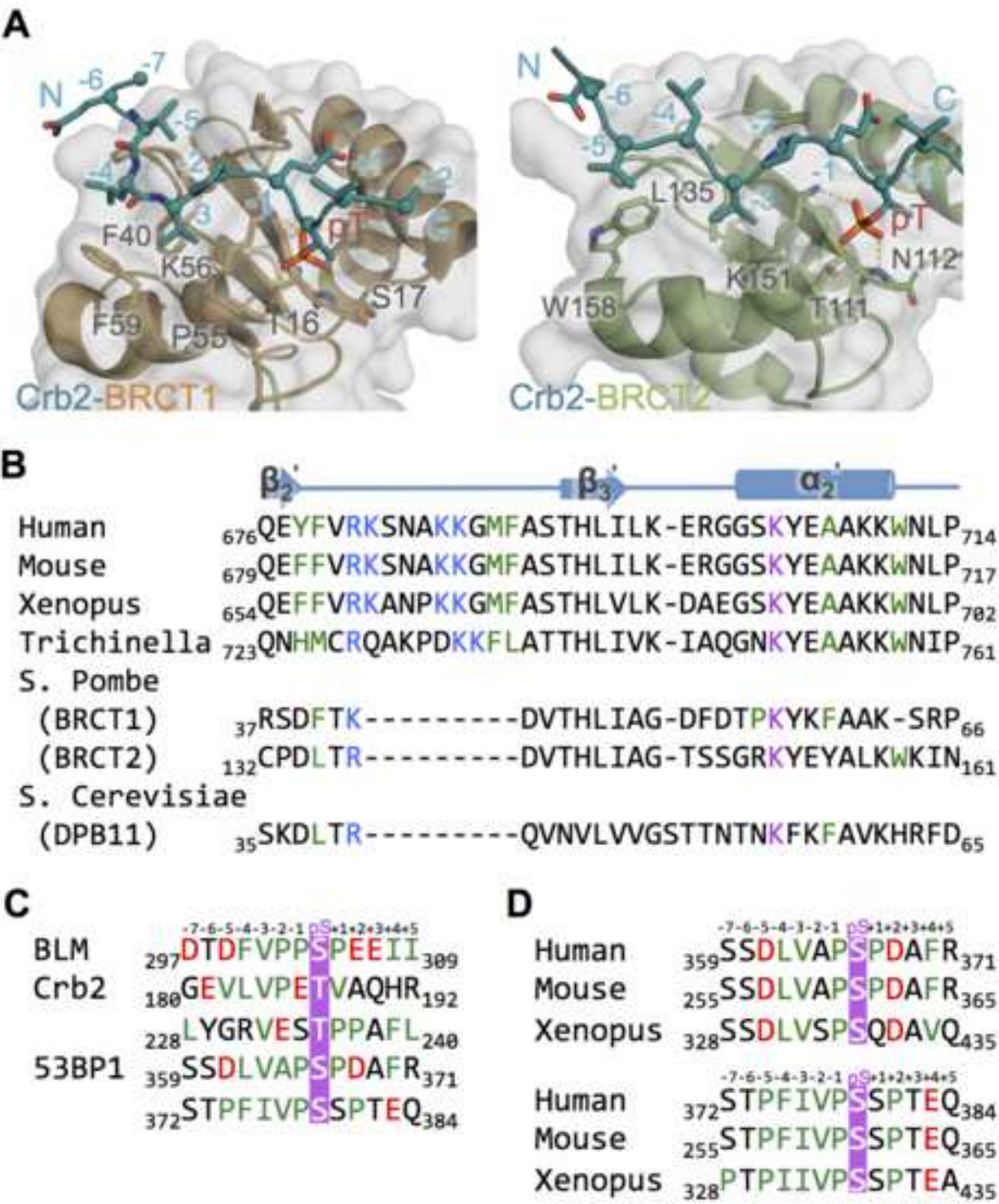


Figure 2

[Click here to download Figure Fig. 2.png](#)



KEY RESOURCES TABLE

REAGENT or RESOURCE	SOURCE	IDENTIFIER
Bacterial and Virus Strains		
BL21 Gold (DE3)	Aligent	Cat# 230132
pGEX6P1	GE Healthcare	Cat# 28954648
Chemicals, Peptides, and Recombinant Proteins		
FITC-DTDFVPPpSPEEII-NH ₂	Genosphere Biotechnologies	N/A
Ac-DTDFVPPpSPEEII-NH ₂	Genosphere Biotechnologies	N/A
Ac-DTDFVPPpSPEEIIKK-NH ₂	Genosphere Biotechnologies	N/A
Ac-DFVPPpSPEEII-NH ₂	Genosphere Biotechnologies	N/A
FITC-KEDVLSTpSKDL-NH ₂	Biomatik	N/A
FITC-GFIDpSDpTDVEEE-NH ₂	Biomatik	Cat# P110628-MJ245934
PreScission protease	Thermo Scientific	Cat# 88946
Lambda protein phosphatase	New England Biolab	Cat# P0753
GST-hTopBP1 BRCT4/5	Leung et al., 2013	N/A
mTopBP1 BRCT4/5	This paper	N/A
hTopBP1 BRCT4/5	Leung et al., 2013	N/A
hTopBP1 BRCT5 Y678A	This paper	N/A
hTopBP1 BRCT5 A707D	This paper	N/A
hTopBP1 BRCT5 A707K	This paper	N/A
hTopBP1 BRCT5 M689A	This paper	N/A
hTopBP1 BRCT5 R681E/K682E	Leung et al., 2013	N/A
hTopBP1 BRCT5 K686E/K687E	Leung et al., 2013	N/A
hTopBP1 BRCT5 K704A	Leung et al., 2013	N/A
Critical Commercial Assays		
QuickChange Lighting site-directed mutagenesis kit	Aligent Technology	Cat# 200519
Deposited Data		
TopBP1 BRCT4/5 – BLM complex structure	This paper	PDB: 5U6K
Software and Algorithms		
DENZO	HKL Research	http://hkl-xray.com/hkl-2000
SCALEPACK	HKL Research	http://hkl-xray.com/hkl-2000
PASHER 25.6	CCP4	http://www.ccp4.ac.uk/html/phaser.html
PyMol 1.8	Schrödinger	www.pymol.org

GraphPad Prism	GraphPad Software	http://www.graphpad.com/scientific-software/prism/
PDB validation server	Protein Data Bank	https://validate-rcsb-1.wwpdb.org/
Other		
Superdex 200 16/60 column resin	GE Healthcare	Cat # 17104301
Superdex 75 26/60 column resin	GE Healthcare	Cat # 17104401
Anion exchange column	GE Healthcare	Cat # 17106601
Glutathione sepharose 4B beads	GE Healthcare	Cat # 17075602

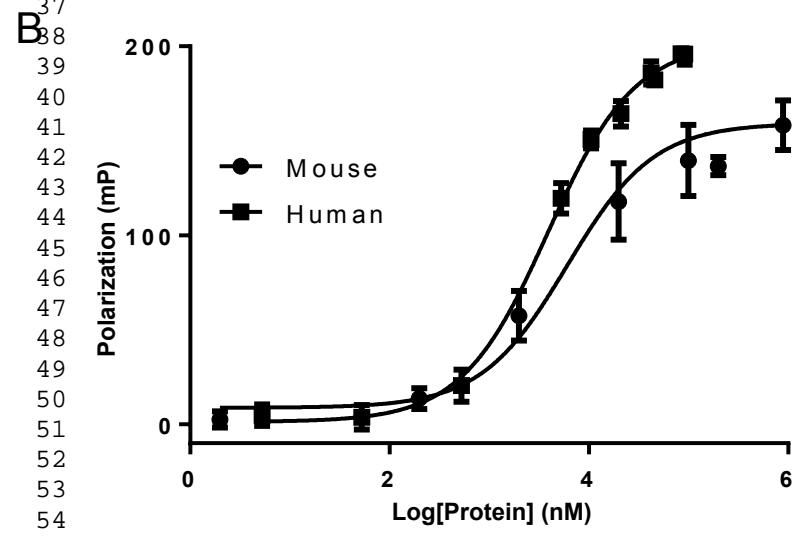
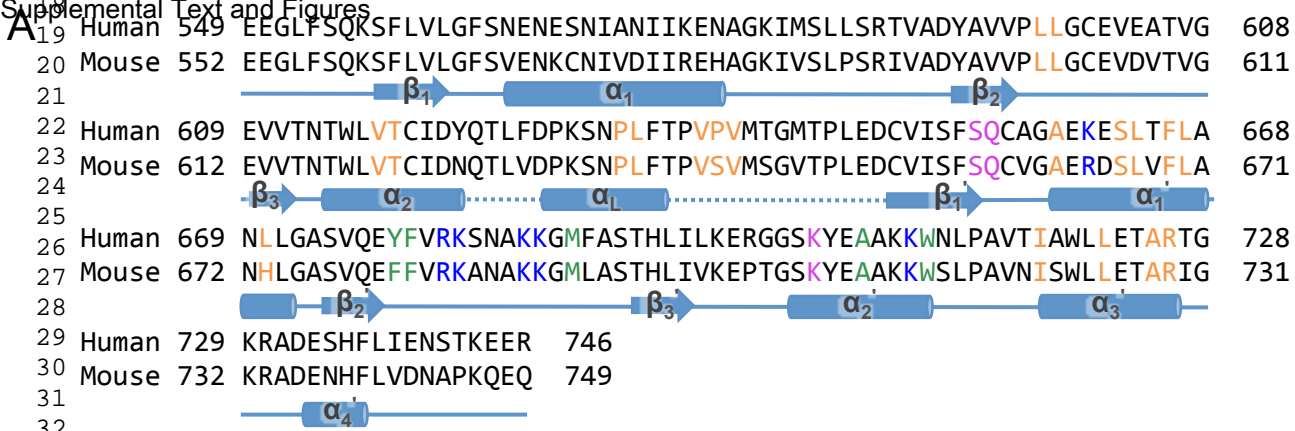
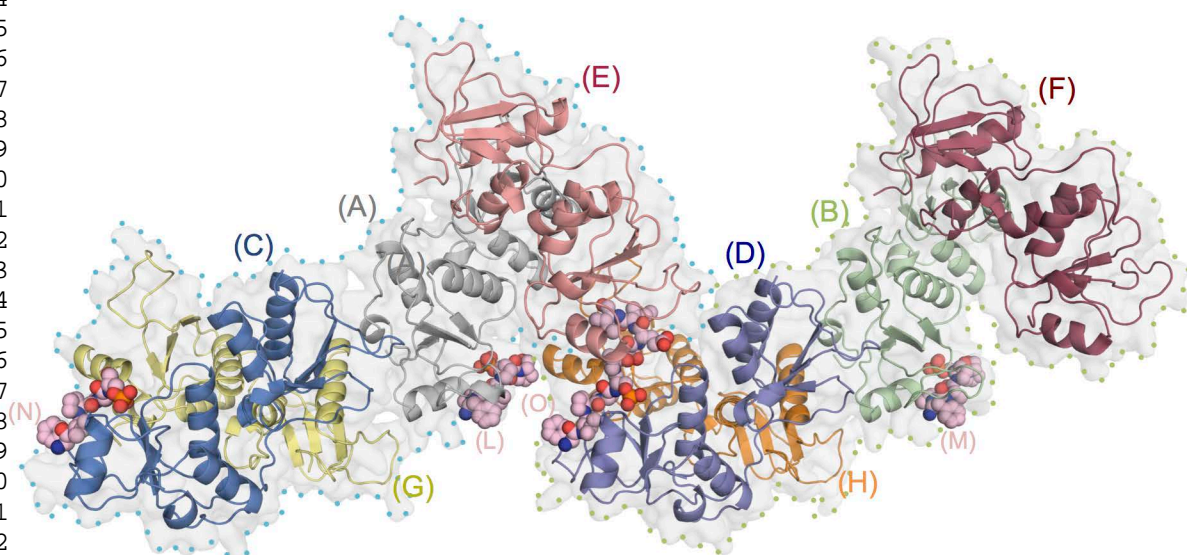
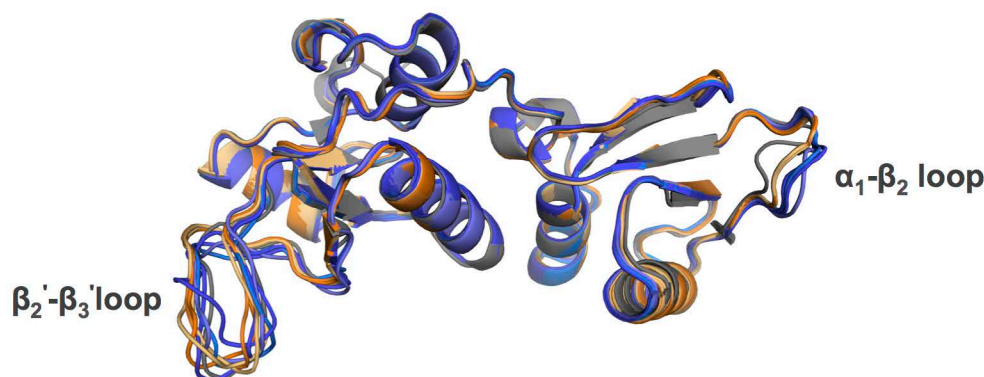


Figure S1. Related to Figure 1. Comparison of human versus mouse TopBP1 BLM interactions.
A Sequence alignment of mouse versus human proteins with secondary structure by PROMALS3D. Residues forming the BRCT-BRCT interface are colored green, residues from the peptide binding surface are colored blue (charged loop), purple (phosphate binding pocket), and orange (hydrophobic groove).
B Comparison of BLM interaction with mouse versus human TopBP1 BRCT4/5 by FP assay.

A



B



C

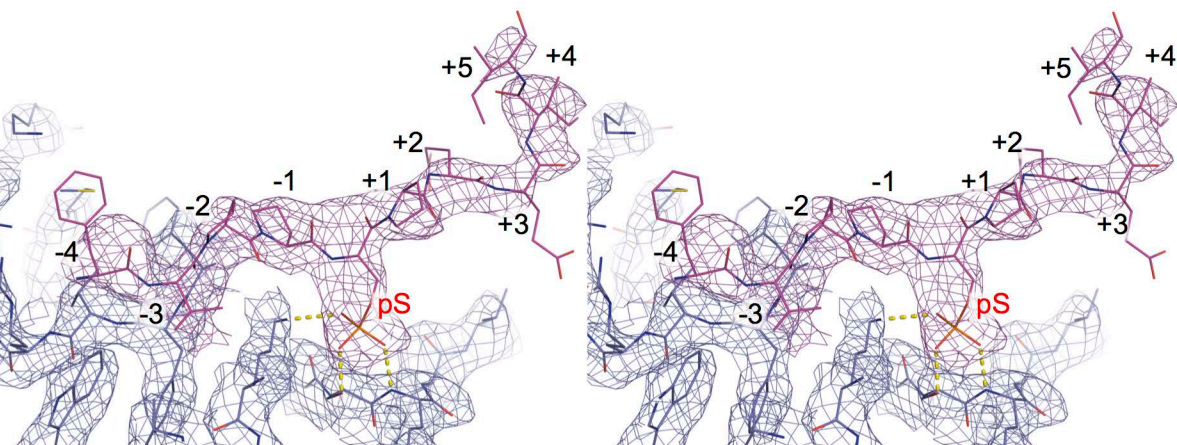


Figure S2. Related to Figure 1. X-ray crystal structure of TopBP1 BRCT4/5 with BLM.

A Overview of the crystallographic asymmetric unit. All BLM peptide chains (L, M, N, O) are in space filling representation (pink). The two groups of protomers that are related by translational symmetry are highlighted with blue and green dotted lines.

B Overlay of all protomers on the structure of human TopBP1 BRCT4/5 (3UEN) in light grey. Peptide bound protomers are in orange hues, apo protomers are in blue hues.

C Representative bias-reduced density map of TopBP1 BRCT4/5 bound to BLM peptide. The stereoview is directed into the peptide-BRCT interface between protomer D and peptide O. Density maps of the peptide (pink) and the BRCT4/5 (blue) are both contoured at 1.0 sigma. The electron density map was calculated using the interact-build omit method.

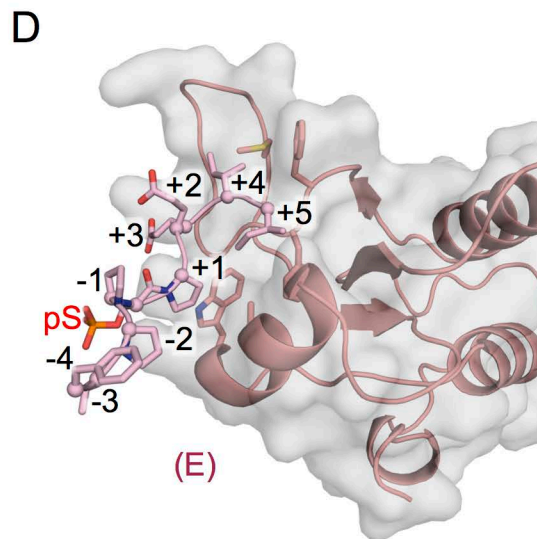
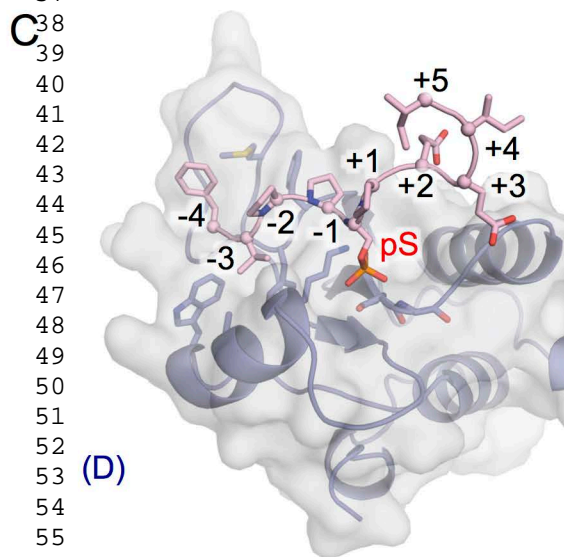
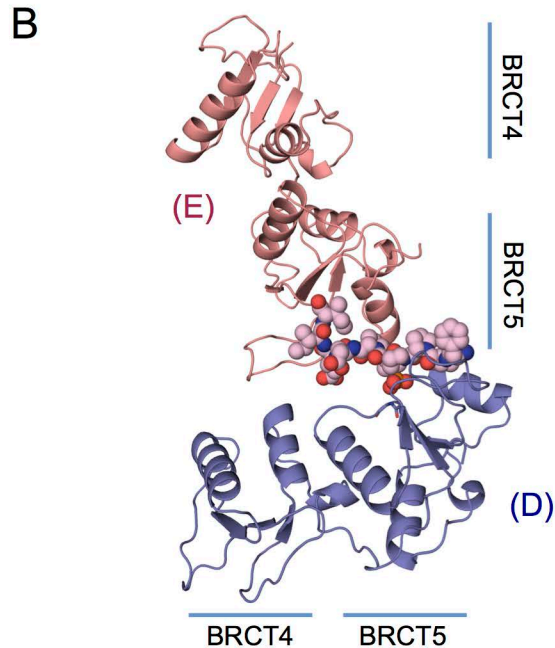
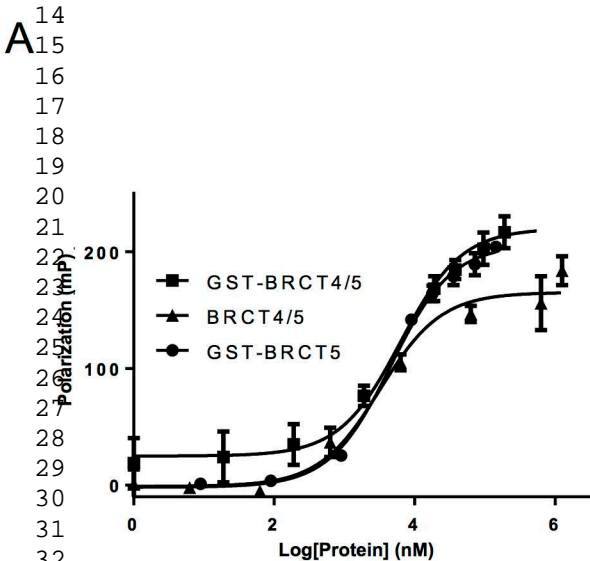


Figure S3. Related to Figure 1. Crystal packing-induced dimer of TopBP1 BRCT4/5 with BLM.

A Interactions of various GST-tagged and non-tagged TopBP1 BRCT constructs with BLM phosphopeptide as assessed by FP.

B Overview of protomer E (salmon) and D (slate) dimerized through peptide O (pink).

C Conserved interaction of BLM with protomer D.

D Packing enforced interaction of BLM with protomer E.

Table S1: Data Collection, Phasing and Refinement Statistics		
TopBP1 BRCT4/5- BLM Complex		
Space group	P 21	
Unit cell dimensions		
a, b, c (Å)	98.16, 96.82, 127.05	
α, β, γ (°)	90, 94.25, 90	
Resolution range (Å) ^a	47.87-2.60 (2.63-2.60)	
No. of unique reflections	71934	
Completeness (%)	98.8	
Overall I/sigma (I)	11.08 (2.65)	
R _{meas} ^b	0.136 (0.920)	
CC _{1/2} ^c	0.970 (0.896)	
R _{free} / R _{work} (%) ^c	25.61/21.93	
Number of atoms	11899	
Wilson B factor (Å ²)	54.87	
Ramachandran Plot (%)		
Most favoured	96.7	
Outlier	0.5	
Clashscore	4.17	
R.M.S. Deviation		
Bonds (Å)	0.003	
Angles (°)	0.546	
^a Values in parentheses are from the highest resolution shell.		
^b $R_{meas} = \frac{\sum_{hkl} \sum_{i=1}^n I_i(hkl) - \bar{I}(hkl) }{\sum_{hkl} \sum_{i=1}^n I_i(hkl)}$		
^c $R_{work/free} = \frac{\sum_{hkl} F_{obs}(hkl) - F_{calc}(hkl) }{\sum_{hkl} F_{obs}(hkl)}$		